SANDIA REPORT
SAND2019-10780
Printed September 2019

Sandia National Laboratories

Mechanical Testing Summary: Optimized Carbon Fiber Composites in Wind Turbine Blade Design

David A. Miller, Daniel D. Samborsky
Montana State University

Brandon L. Ennis
Sandia National Laboratories

Prepared by
Sandia National Laboratories
Albuquerque, New Mexico
87185 and Livermore,
California 94550

Issued by Sandia National Laboratories, operated for the United States Department of Energy by National Technology & Engineering Solutions of Sandia, LLC.

Available to DOE and DOE contractors from
U.S. Department of Energy
Office of Scientific and Technical Information
P.O. Box 62
Oak Ridge, TN 37831

Telephone: (865) 576-8401
Facsimile: (865) 576-5728
E-Mail: reports@osti.gov
Online ordering: http://www.osti.gov/scitech

Available to the public from
U.S. Department of Commerce
National Technical Information Service
5301 Shawnee Rd
Alexandria, VA 22312

Telephone: (800) 553-6847
Facsimile: (703) 605-6900
E-Mail: orders@ntis.gov
Online order: https://classic.ntis.gov/help/order-methods/

ABSTRACT

The objective of the Optimized Carbon Fiber project is to assess the commercial viability to develop cost-competitive wind-specific carbon fiber composites to enable larger rotors for increased energy capture. Although glass fiber reinforcement is the primary structural material in wind blade manufacturing, utilization of carbon fiber has been identified as a key enabler for achieving larger rotors because of its higher specific stiffness (stiffness per unit mass), specific strength (strength per unit mass), and fatigue resistance in comparison to glass. This report contains the testing process and results from the mechanical characterization portion of the project. Low-cost textile carbon fiber materials are tested along with a baseline, commercial carbon fiber system common to the wind industry. Material comparisons are made across coupons of similar manufacturing and quality to assess the properties of the novel carbon fibers.

ACKNOWLEDGEMENTS

This work has been funded by the United States Department of Energy Wind Energy Technologies Office as part of the Optimized Carbon Fiber Composites for Wind Turbine Blades project.

The authors would also like to recognize the contributions of project member Bob Norris at Oak Ridge National Laboratory in identification of the low-cost carbon fiber materials studied, in addition to his work with a commercial pultruder to produce the third-party pultrusions tested within this study.

CONTENTS

LIST OF FIGURES

LIST OF TABLES

ACRONYMS AND DEFINITIONS

Abbreviation	Definition
DOE	Department of Energy
MSU	Montana State University
SNL	Sandia National Laboratories
ORNL	Oak Ridge National Laboratory
CFTF	Carbon Fiber Technology Facility
LCCF	Low Cost Carbon Fiber
LCOE	Levelized Cost of Energy
UTS	Ultimate Tensile Strength
UCS	Ultimate Compressive Strength
E	Elastic Modulus
R	Fatigue Stress Ratio
V_F	Volume Fraction
SEM	Scanning Electron Microscope

1. INTRODUCTION

Carbon fiber composites offer significantly enhanced mechanical properties compared to glass fiber composites, enabling the design and manufacture of larger, higher energy capture rotors. However, carbon fiber materials are much more costly than glass fiber, hindering their broader adoption in wind turbine blades. Carbon fiber composites were originally designed and applied to military and aerospace applications where cost was not a primary driver. Thus, significant opportunities may exist to reduce the overall cost of incorporating carbon fiber materials into wind turbine blades, which are heavily impacted by cost. These opportunities range from changing the raw input materials, fiber conversion processes, and formats of the carbon fiber itself, through the composite material forms (e.g. pultrusion, prepreg) used in the blade manufacturing process.

The magnitude of this cost reduction opportunity has been quantified through the U.S. Department of Energy's Optimized Carbon Fiber Composites for Wind Turbine Blades project [1]. This project has assessed baseline and novel carbon fiber materials through material cost estimation, mechanical testing, and, ultimately, through blade structural optimizations using the defined materials. The present report summarizes work performed in the mechanical characterization portion of the project, and details the processing, testing procedures, and test results.

1.1. Background and Motivation

It is clear from wind turbine design trends that existing, commercial carbon fiber materials have properties which are important for enabling the longer wind turbine blades being designed and the continued reductions in levelized cost of energy (LCOE) expected. However, the economics do not appear to work out as favorably for smaller machines to justify the improved mechanical properties of existing carbon fiber materials in these blade designs. Market trends towards longer blades and larger machines will drive demand for carbon fiber blade designs. Without further innovation, carbon fiber will continue to be utilized only in certain wind turbine designs and may hinder the development of wind turbines in low wind resource sites or of certain sizes.

The objective of the Optimized Carbon Fiber project is to assess the commercial viability to develop cost-competitive carbon fiber composites to enable larger rotors for increased energy capture. Utilization of carbon fiber has been identified as a key enabler for achieving larger rotors because of its higher specific stiffness (stiffness per unit mass), specific strength (strength per unit mass), and fatigue resistance in comparison to fiberglass. Carbon fiber is currently being used in some wind turbine blades, exclusively in spar caps; however, more wide-spread utilization of carbon fiber is very much dependent on demonstrating a compelling business case. The objective of this project is to identify and compare different material approaches and requires material test article fabrication and mechanical testing.

Through analysis of commercial carbon fiber and novel low-cost carbon fiber materials, the results will be useful to identify important steps in development of more optimal carbon fiber materials for wind turbine spar caps, considering material cost and relevant mechanical property relationships. The initial considerations of test articles and configurations within this study focus on uniaxial coupon characterization to represent spar cap composites, although it is expected that the results of the project may have implications for other parts of wind blades.

2. SUMMARY OF MECHANICAL CHARACTERIZATION

2.1. Carbon Fiber Study Material Definition

The Department of Energy (DOE) has supported development of low or lower cost carbon fiber at Oak Ridge National Laboratory (ORNL) for well over a decade. This Low-Cost Carbon Fiber (LCCF) Program has demonstrated a variety of approaches from radical changes to precursor chemistry, to looking at more cost-effective forms of acrylic fibers, to employing advanced conversion techniques using plasma and/or microwave heating. The prior work is leveraged by the current study to analyze the effectiveness of the novel low-cost materials for use in wind turbine blades. Wind turbine blades of current sizes see the greatest loading in the flap (or thrust) direction and the main structural members which carry this load are the spar caps. For this reason, the present work focuses on testing results of most importance to blade spar caps. Spar caps consist of mostly uniaxial fibers with transverse loads typically carried by biaxial materials in the blade shell. In the case of carbon fiber spar caps, intermediate pultruded composites are being considered as the only composite form for usage in wind turbine blade spar caps. This is due to the small diameter carbon fiber having poor resin flow characteristics in infusions and the increased sensitivity to manufacturing on the overall composite performance.

The mechanical testing focuses on longitudinal properties of importance to wind turbine spar caps, e.g., uniaxial composite tensile and compressive strength and stiffness. Pultruded composite sheets are the most ideal form for carbon fiber usage in wind turbine spar caps, however, this manufacturing process requires significant optimization to yield representative material results. For this reason, a secondary composite form has been developed as part of this work, the Montana State University (MSU) aligned strand infusion, described in Section 3.1. The aligned strand infused composites are studied to enable direct material comparison while limiting testing bias incurred from composite manufacturing. Commercial pultruded samples are also studied, where available, to understand the effect of the optimized composite manufacturing process on the material properties. Additionally, third-party pultruded composite samples were manufactured as part of this project to test each of the study materials in pultruded composite forms for comparison. This proved to be inconclusive due to the difficulty of obtaining the high fiber volume fractions needed to prevent dry spots and voids in the composite. A summary of tested composite forms and the objective of each study is presented in Table 2-1.

Table 2-1. Tested composite forms and objective description.

Composite form	Testing objective
MSU aligned strand infusion	Controlled process designed to minimize manufacturing bias and enable direct material comparison
Commercial pultrusion	Most representative process for commercial wind turbine blade spar cap material, used to understand the relative performance compared to MSU aligned strand infusions
Third-party pultrusion	Performed to identify if additional difficulties arise from pultruding the heavy-tow materials compared to the industry baseline, should not be used for actual mechanical performance

Three carbon fiber materials are studied to compare developmental low-cost materials with an industry baseline material which is commonly utilized by wind turbine designs with carbon fiber spar caps, Zoltek PX35 carbon fiber. The low-cost carbon fiber materials were developed by the Carbon Fiber Technology Facility (CFTF) at ORNL and use two different heavy-tow textile precursors,

Taekwang and Kaltex. The supplied dry carbon tow materials and their respective lot numbers are detailed in Table 2-2.

Table 2-2. Carbon fiber study materials.

Dry fiber inputs	Roll labels	Tow fiber count
Taekwang T20C (low-cost)	TE3631170205 / TE3631170501	363K tow
Kaltex K20-HTU (low-cost)	TE4571150808 / TE4571180605	457K tow
Zoltek PX3505015T-13 (industry baseline)	SN 22224094, lot 4C22-6076	50K tow

The study materials were manufactured into pultruded composite forms outside of Montana State University. Within the project, the three materials were all manufactured in third-party pultruded composite forms by Martin Pultrusion. The Zoltek PX35 material is also studied using the commercially available pultruded composite plate from Zoltek. These tested unidirectional pultruded plates are listed in Table 2-3. Manufacturing process details on these pultruded materials are not included in the scope of this testing program; however, relevant material properties, such as microstructure and fiber volume fraction are listed.

Table 2-3. Pultruded composite test forms and nomenclature.

Label nomenclature	Fiber	Pultrusion	Supplied form
112017-4, 112017-5 (Kaltex pre-cursor)	K20-HTU	Third-party	50 mm wide x 3.5 mm thick
112017-6 (Zoltek)	PX-35	Third-party	
FCE2.0-200, 5T10-7017 (Zoltek)	PX-35	Commercial	205 mm wide x 1.87 mm thick

2.2. Summary of Material Testing Results

Table 2-4 includes all the testing results on materials listed above. Results are grouped from a single manufacturing process, e.g., test results from separately manufactured coupons are listed separately. Note that these results represent limited sample numbers, with non-optimized matrix materials, fiber forms, or manufacturing processes. Therefore, it is not unexpected that commercial pultruded components from the control fiber manufacturer (PX35) yielded the highest performance. Details on coupon manufacturing and testing are included in later sections of this report.

The table includes data from early testing iterations which followed testing standards, but with procedures that had yet not been optimized to remove testing bias (especially in compression). As an example, the Zoltek pultruded plate in early compression tests without the more optimized testing procedure (including tabs) resulted in failures near the test grips and significantly lower strength values than the optimized procedure developed through this test campaign (UCS values of -880 vs. -1505 MPa, respectively). These data are both included to bring attention to the difficulty of compressive tests and the large variance based on testing protocols used. Additionally, the compressive tests reported for the Zoltek PX35 aligned strand composites resulted in lower strengths than expected (-906 MPa), which is likely due to a sub-optimal composite manufacturing process. The third-party pultruded composites produce lower values than expected for each of the tested materials due to the lack of optimization of the manufacturing, as explained previously.

Table 2-4. Summary of properties for the three fiber cases (averages from test series with sample standard deviations shown in brackets).

Material	Layup	V_F, %	E, GPa 0.1-0.3%	UTS, MPa	%, max	UCS, MPa [1]	%, min
Zoltek PX35 MSU Infused	Single tow	52	126 [10]	2193 [67]	1.59 [0.04]		
	5.1 tows/cm	51	119 [4]	1726 [93]	1.4 [0.08]		
	[0]	51				-906 [44]	-0.74 [0.04]]
Zoltek PX35 Third-party pultruded	[0], 112017-6	53	114 [4]	1564 [67]	1.33 [0.15]	-897 [67]	-0.79 [0.06]
Zoltek FCE2.0-200	[0]	62	142 [3] 138 [9]	2215 [77]	1.5 [0.10]	-1505 [38] -880 [37]	-1.21 [0.05] -0.63 [0.04]
	[90]	62	9.13 [0.12]	50.1 [8]	0.58 [0.11]		
ORNL T20-C MSU Infused	$[0]_3$	49	126 [4]	968 [54]	0.75 [0.05]		
	$[0]_5$	52	121 [5]	978 [41]	0.78 [0.04]		
	$[0]_{10}$	52	124 [13]			-573 [30]	-0.47 [0.07]
	$[90]_5$	52	7.8 [0.6]	31.7 [4]	1.13 [0.08]		
	$[0/90]_{3S}$	50	67.4 [0.8]			-475 [22] -893 [41] [A]	-0.73 [0.05]
	$[0]_5$ Tension $[0]_{20}$ Comp.	50	126 [4]	956 [63]	0.74 [0.05]	-869 [46]	-0.69 [0.04]
ORNL K20-HTU Third-party pultruded	[0], 112017-4	51				-803 [26]	-0.65 [0.02]
	[0], 112017-5	51	123 [6]	846 [53]	0.69 [0.05]	-769 [73]	-0.63 [0.06]
ORNL K20 MSU Infused	$[0]_5$ Tension $[0]_{20}$ Comp.	47	112 [6]	990 [49]	0.84 [0.06]	-863 [108]	-0.77 [0.10]

[1] Compressive testing followed a modified ASTM D6641 method. [A] UCS was calculated using a back-out factor method.

3. DETAILED MECHANICAL TESTING RESULTS

3.1. Composite Form Manufacturing Description

Laminates were constructed from the supplied Zoltek PX35 (PX3505015T-13) tows using the flat plate winding method, shown in Figure 3-1. Plate winding with the larger tows (T20C, K20) was not possible, so direct tow cutting and stacking on a flat mold was done, as shown in Figure 3-2 and Figure 3-3. During this process, the tows are held in tension during stacking and assembly using a taping process to ensure alignment of tows during the infusion process. These preforms were then infused using a typical vacuum infusion setup detailed in Figure 3-4. The resin system used was an epoxy (Hexion 135/1366) and initially cured at room temperature for 24 hours, followed by a post cure of 12 hours at 70°C.

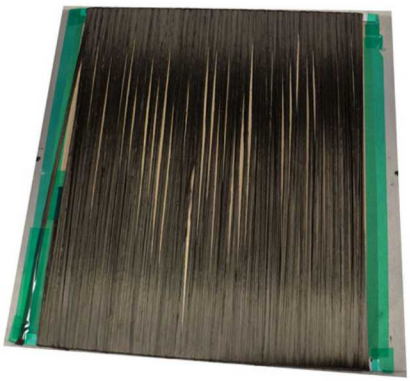

Figure 3-1. Typical tow winding detailing tow separations on the 5.1 tows/cm Zoltek PX35 laminate (45 cm x 45 cm plate dimensions).

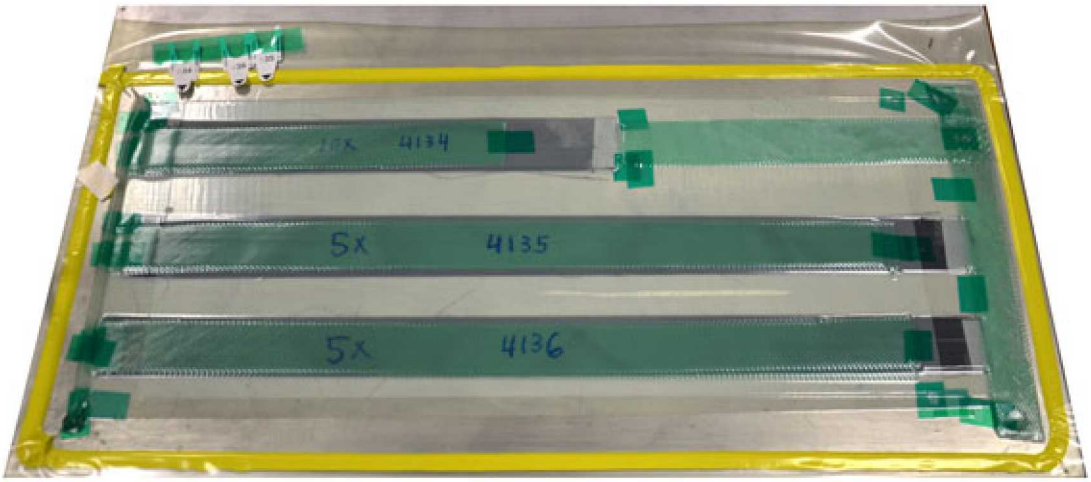

Figure 3-2. Infusion of $[0]_5$ and $[0]_{10}$ ORNL LCCF laminates on a 76 cm long flat plate.

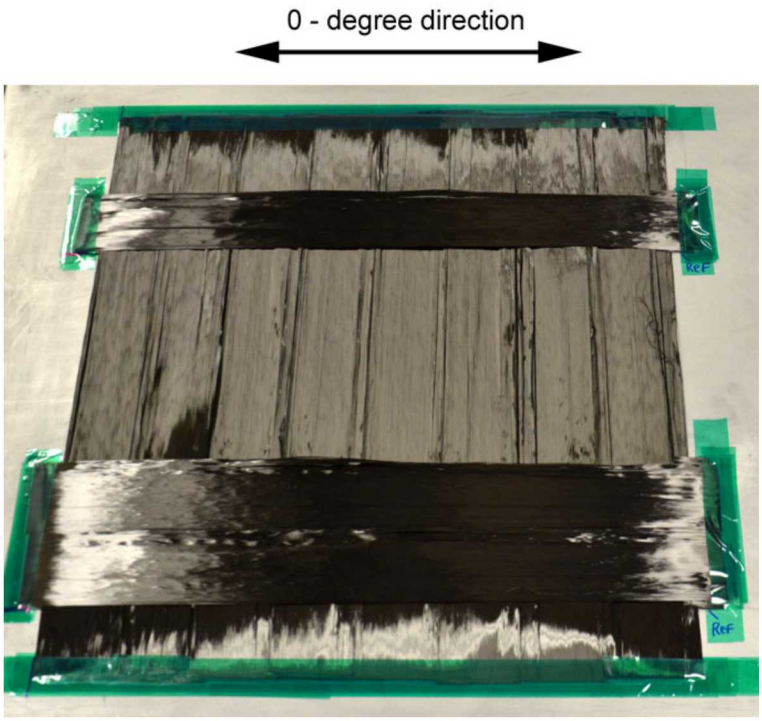

Figure 3-3. Infusion of $[0/90]_{3S}$ and $[90]_5$ ORNL LCCF laminates, 45 cm x 45 cm plate dimensions.

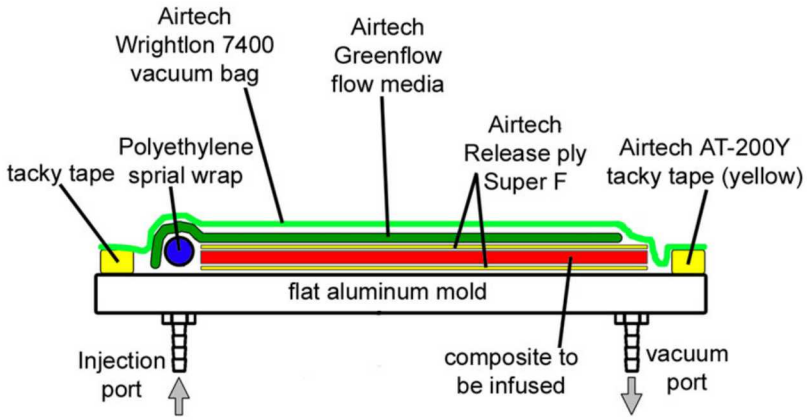

Figure 3-4. Typical vacuum infusion plate details.

The fiber volume fraction was calculated from fiber input weights and confirmed using scanning electron microscope (SEM) micrographs. Fiber volume fractions of the vacuum infused plates were approximately 50% as broken fibers inhibited the fiber stack from condensing. This can be seen in Figure 3-5 with the Taekwang coupon, T20-456 on the right, showing a white matrix line region going top to bottom in the 500X SEM micrograph. The SEM micrographs also concluded that the porosity content was negligible in the MSU infused laminates.

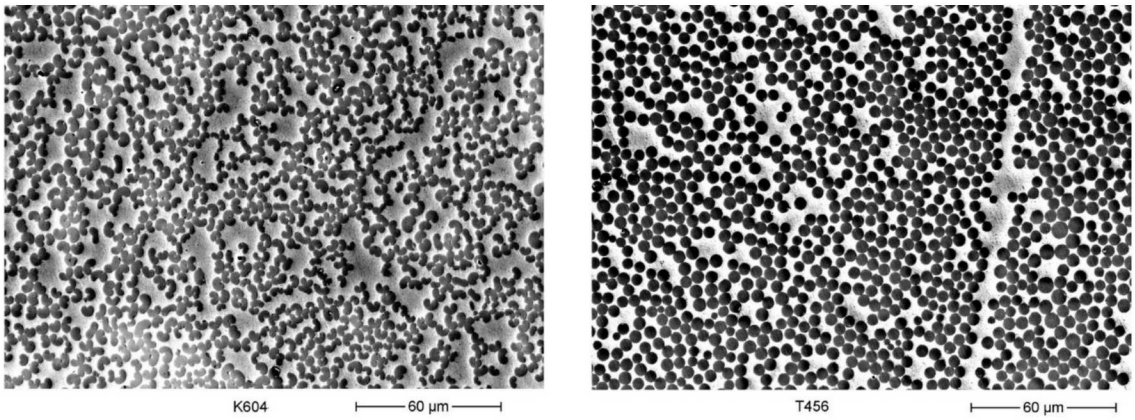

Figure 3-5. SEM micrographs of the Kaltex fiber coupon (coupon K20-604, left) and the Taekwang fiber coupon (coupon T20-456, right) detailing the fiber distributions in the MSU infused laminates. (carbon fibers are shown black with the white surrounding epoxy matrix).

All composite plates were sectioned using a standard water-cooled tile saw with a continuous diamond coated rim blade. Test coupons with thru-thickness surface waviness and higher strength unidirectional materials required fiberglass G10 end tabs bonded to the surface to prevent gripping damage.

Transverse direction testing (90°) did not require additional end tabs for acceptable tensile failures. Armstrong A12 (1:1 weight mix) epoxy was used for bonding on the end tabs and room temperature cured for 3 days at 23-28°C prior to testing.

Typical tensile and compressive test coupon geometries are detailed in Figure 3-6. Coupon dimensions were measured for cross sectional areas in the gage length using a NIST calibrated Mitutoyo 500-474 CD-S6-CT Digimatic digital caliper, with a minimum resolution and accuracy of 0.01 mm. Micro-Measurements C2A-13-250LW-120 (2.100 gage factor) strain gages were applied to some of the static test coupons with M-Bond 200 cyanoacrylate adhesive and cured at room temperature for 24 hours. All tensile coupons not strain gaged, utilized an Instron 2620-824 series clip-on extensometer with a gage length of 25 mm. The elastic modulus was calculated from the best fit stress-strain slope between the strain values of 0.1% to 0.3% strain.

3.1.1. Testing Protocols

Tension tests were performed on two Instron testing machines, an 8562 (100 kN capacity, servo-electric) and an 8802 (250 kN capacity, servo-hydraulic). Both test frames employed hydraulic wedge grips with anti-rotation and anti-lateral translation devices. All equipment used in these tests followed ASTM standards (E4 (force), E74 (force), E83 (extensometers), E251 (strain gages) in regard to accuracy, alignment, calibration and operation [2-5]. All static tests were performed at a displacement rate of 0.0254 mm/s. Tests were at ambient room temperatures, 19 to 26°C, and 18 - 36% relative humidity's at Montana State University in Bozeman, Montana. Additional details on material testing hardware and procedures are documented in Mandell et al. [6].

Tensile testing 100% unidirectional laminates is always a challenge as the stress concentrations in the gripped ends of the test coupon promote failures outside the gage section. Traditional width tapering to reduce the cross-sectional area in the gage section does not work. Standard ASTM D3039, 12.6 mm wide test coupons were thickness tapered, where possible, to try to get better gage

section failure modes, as shown in Figure 3-6. The method of thickness tapering is similar to placing tabs on the rectangular coupon, but experience has shown that the tapering produces more representative ultimate strengths and better gage section failures. The bonding of additional G10 tabs was done on coupons without any thickness tapering. Some of the third-party pultruded laminates had large dry fiber areas and high porosity which excluded them from being mechanically tested and are shown in Figure 3-7.

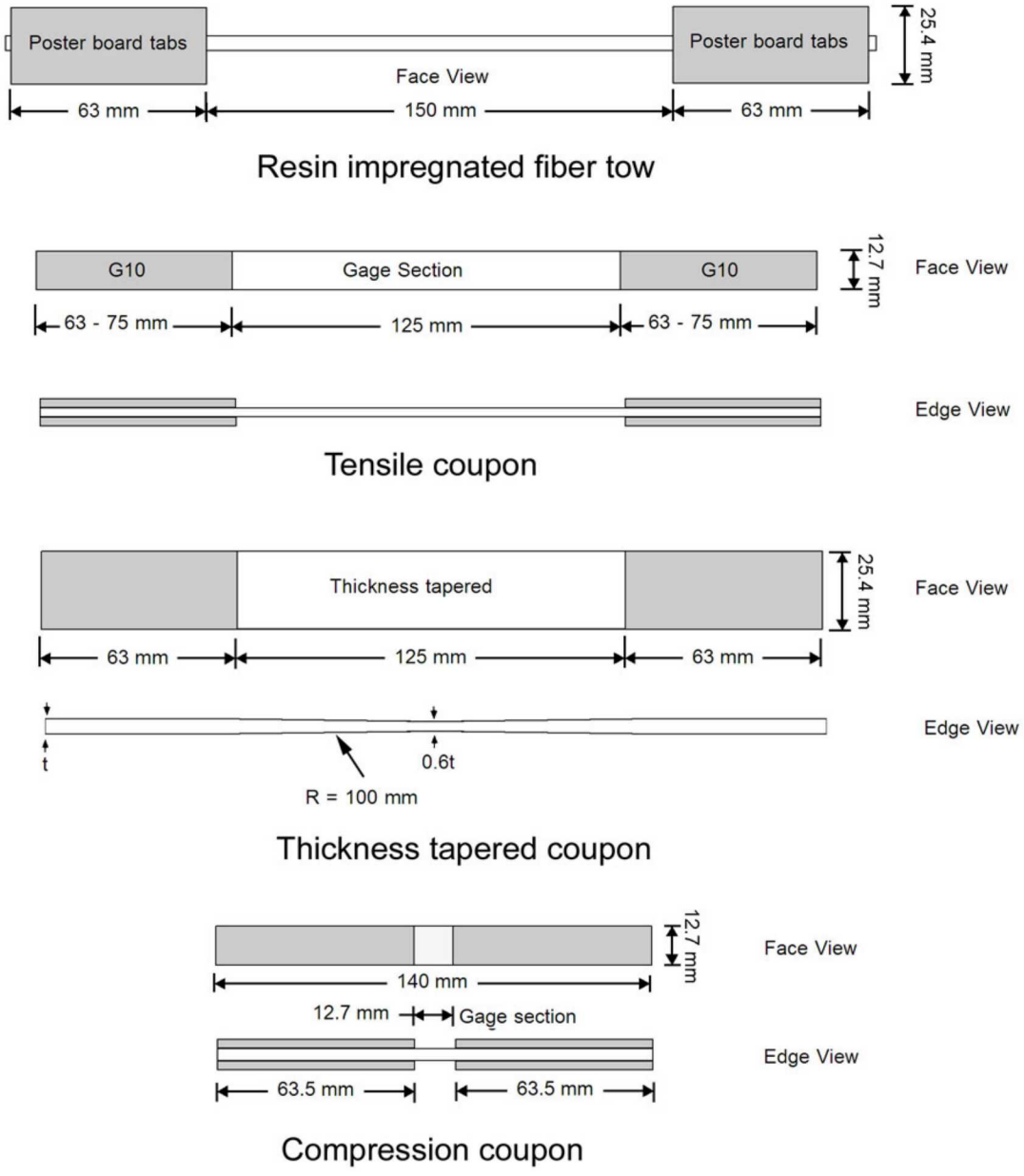

Figure 3-6. Typical test coupon geometries.

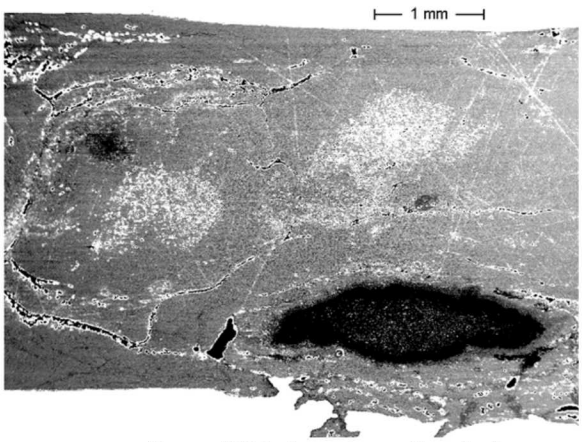

Figure 3-7. 20X full thickness cross-section of third-party pultruded coupon illustrating large areas with dry carbon tows.

Compressive testing of materials is often a difficult and a controversial process as premature failure or buckling of the coupon will undermine the test. ASTM test method D6641 [7] was selected as the best method to get the compressive properties of the unidirectional carbon laminates, as it uses combined end and shear loading to introduce loads into the 12.7 mm gage section. In order to confirm some of the testing procedures, one test series used a $[0/90]_{3S}$ layup and the unidirectional strength was calculated (or backed-out) with standard laminate analysis techniques (Back-out factor = $2E_{11}/(E_{11} + E_{22})$). These strengths were then compared with the 100% unidirectional tests. It was decided early in the testing program that the D6641 method used was to compare mechanical compressive properties of the control carbon fiber group to the two LCCF fiber groups in a quality control type of procedure. With the limited amount of test material, a full test development of the best compression test procedure and geometry for the materials was not performed. Following the initial D6641 test results, the PX35 carbon fiber control group strength was regarded as low, so the ASTM test method was modified with higher clamping bolt torques (11 N-m) and no secondary end milling on the standard coupons for all three fiber cases. Higher clamping pressures can promote early gripping failures due to poissonic thickness expansion of the material as it exits the gripping steel fixture. With a gage length of 12.7 mm the column slenderness ratio, SR, can be calculated by: SR = 3.46 x (gage length /thickness). Various publications indicate that a slenderness ratio less than 30 is not prone to buckling failure, which indicated that the compression tested thickness should be greater than 1.5 mm.

Fatigue tests were run under load control, constant amplitude in a tension-tension condition with R = 0.1. The test frequency was typically between 1-3 Hz and specimen surfaces were air cooled with fans to avoid heating of more than a few °C. For the fatigue test results, the strains given are initial strains measured on the first few cycles. These strain values are lower than those which will accumulate during the fatigue lifetime; however, the strain is the more general parameter for material comparison. Stress plots are sensitive to laminate construction (% 0-degree plies) and fiber content differences when comparing materials.

3.2. Mechanical Test Results

3.2.1. Zoltek PX35 Static Test Results

Figure 3-8 through Figure 3-10 show the stress-strain results for all forms of the PX-35 fiber system. All manufacturing methods show a very linear deformation in tensile loading until the maximum stress is reached. However, a distinct non-linearity is seen in the compressive tests.

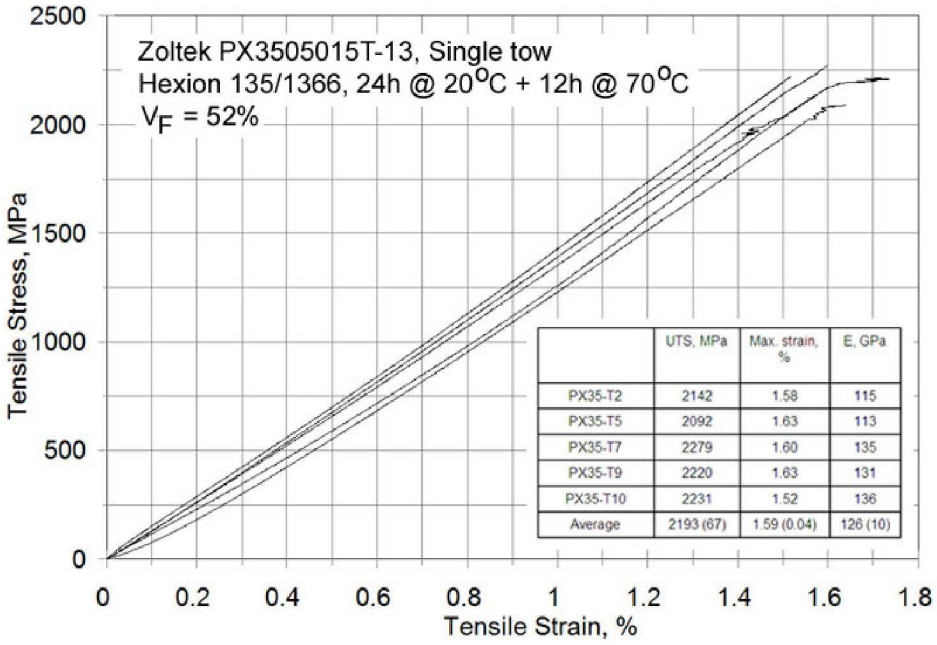

	UTS, MPa	Max. strain, %	E, GPa
PX35-T2	2142	1.58	115
PX35-T5	2092	1.63	113
PX35-T7	2279	1.60	135
PX35-T9	2220	1.63	131
PX35-T10	2231	1.52	136
Average	2193 (67)	1.59 (0.04)	126 (10)

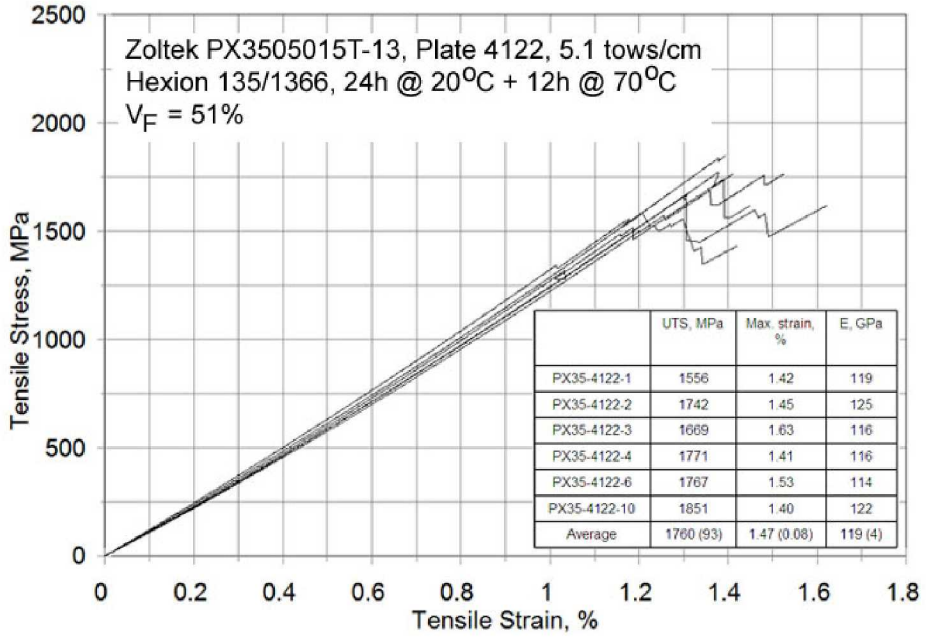

	UTS, MPa	Max. strain, %	E, GPa
PX35-4122-1	1556	1.42	119
PX35-4122-2	1742	1.45	125
PX35-4122-3	1669	1.63	116
PX35-4122-4	1771	1.41	116
PX35-4122-6	1767	1.53	114
PX35-4122-10	1851	1.40	122
Average	1760 (93)	1.47 (0.08)	119 (4)

Figure 3-8. Summary of the Zoltek PX35 single tow and 5.1 tows/cm plate tension tests.

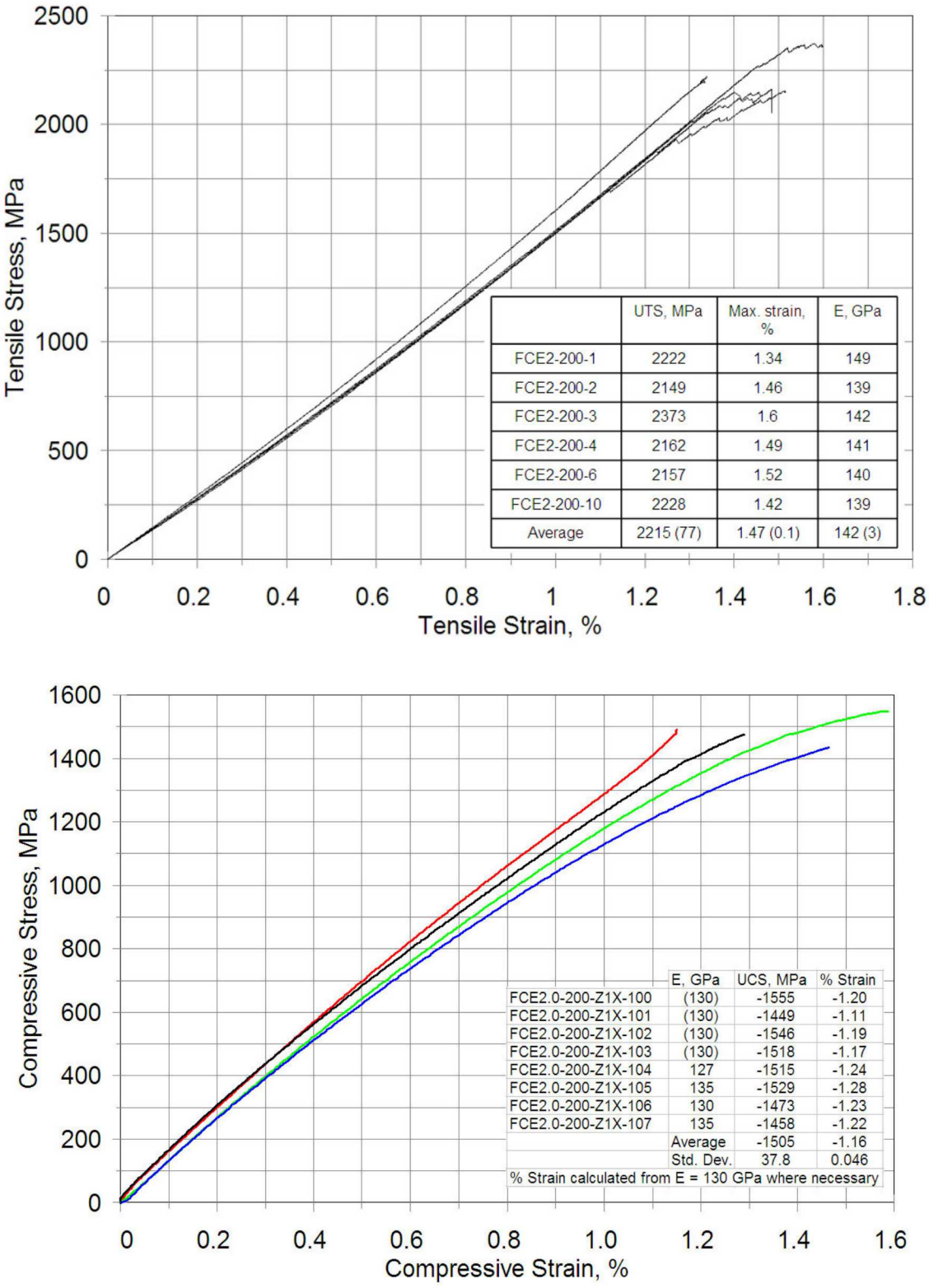

	UTS, MPa	Max. strain, %	E, GPa
FCE2-200-1	2222	1.34	149
FCE2-200-2	2149	1.46	139
FCE2-200-3	2373	1.6	142
FCE2-200-4	2162	1.49	141
FCE2-200-6	2157	1.52	140
FCE2-200-10	2228	1.42	139
Average	2215 (77)	1.47 (0.1)	142 (3)

	E, GPa	UCS, MPa	% Strain
FCE2.0-200-Z1X-100	(130)	-1555	-1.20
FCE2.0-200-Z1X-101	(130)	-1449	-1.11
FCE2.0-200-Z1X-102	(130)	-1546	-1.19
FCE2.0-200-Z1X-103	(130)	-1518	-1.17
FCE2.0-200-Z1X-104	127	-1515	-1.24
FCE2.0-200-Z1X-105	135	-1529	-1.28
FCE2.0-200-Z1X-106	130	-1473	-1.23
FCE2.0-200-Z1X-107	135	-1458	-1.22
	Average	-1505	-1.16
	Std. Dev.	37.8	0.046

Figure 3-9. Tensile and compressive test summary of the Zoltek supplied FCE2.0-200 pultruded PX35 plates (V_F = 62%).

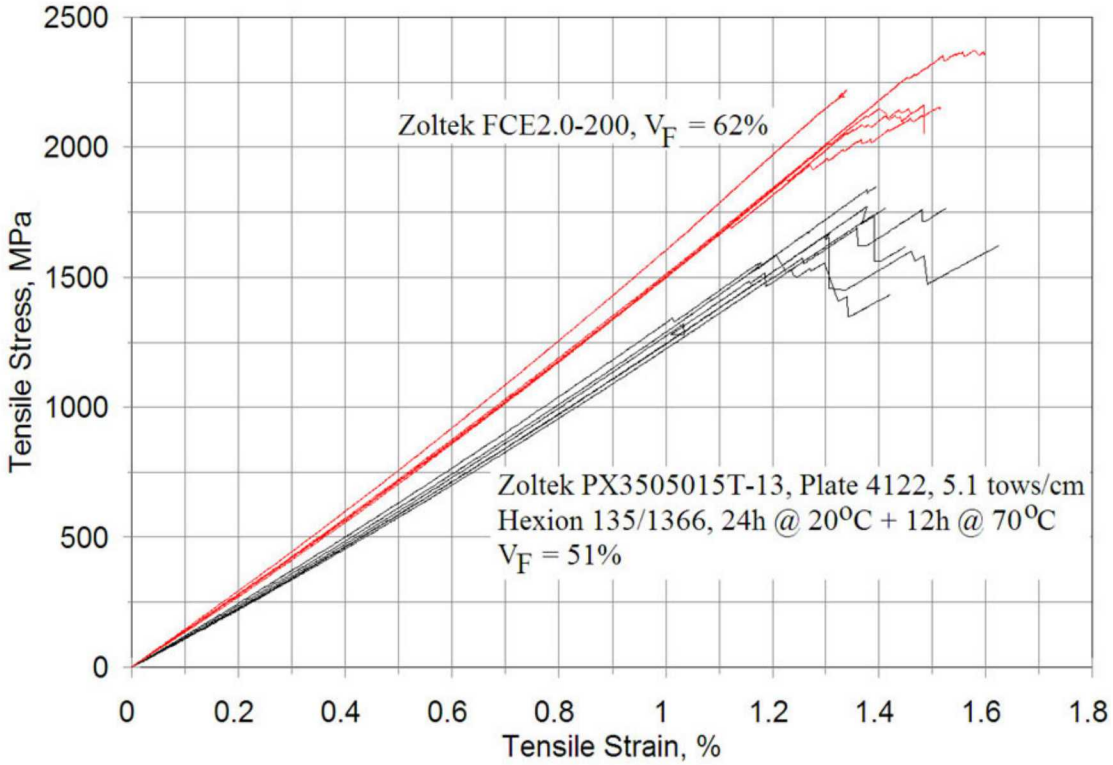

Figure 3-10. Summary of the MSU infused PX35 plate versus the supplied pultruded plates (differences are partially due to fiber volume fraction differences).

3.2.2. Taekwang T20 Static Test Results

Figure 3-11 through Figure 3-13 show static stress-strain results for the Taekwang precursor composites. A unique element seen in these coupons is the apparent lack of any damage, or stiffness loss, before final fracture. One interpretation of this fact could be poor damage tolerance of the material system. Further testing could investigate this phenomenon in future tests, as well as the unique fracture pattern of the coupons.

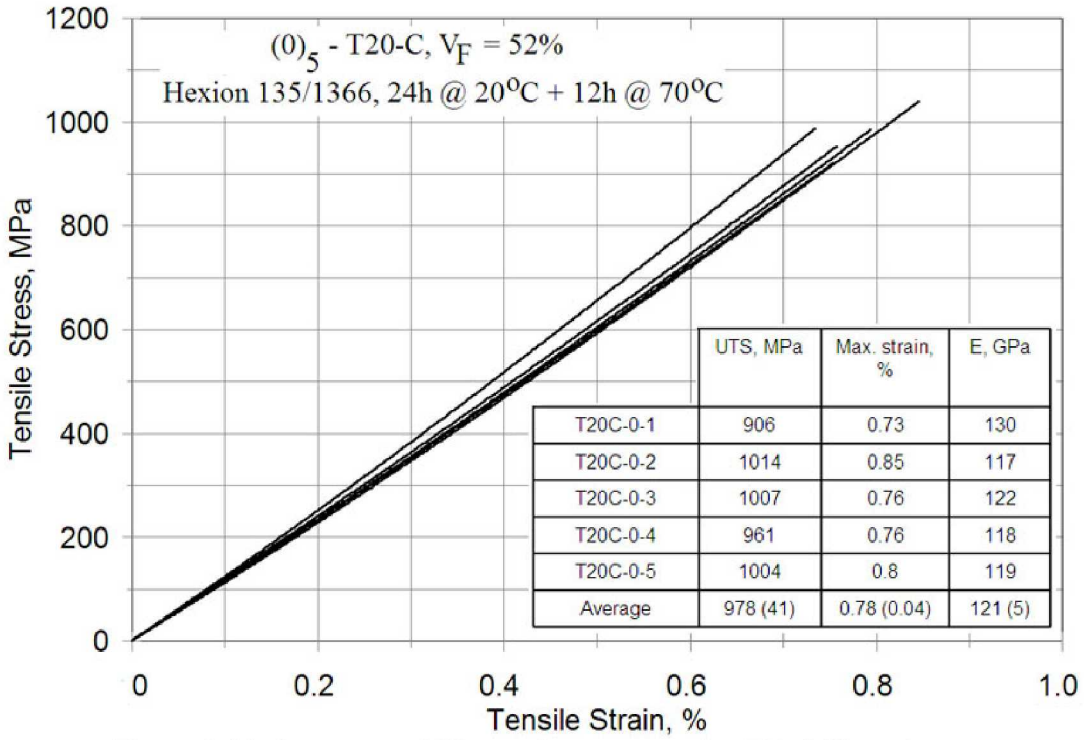

	UTS, MPa	Max. strain, %	E, GPa
T20C-0-1	906	0.73	130
T20C-0-2	1014	0.85	117
T20C-0-3	1007	0.76	122
T20C-0-4	961	0.76	118
T20C-0-5	1004	0.8	119
Average	978 (41)	0.78 (0.04)	121 (5)

Figure 3-11. Summary of $[0]_5$ tension tests on the T20-C fiber plates.

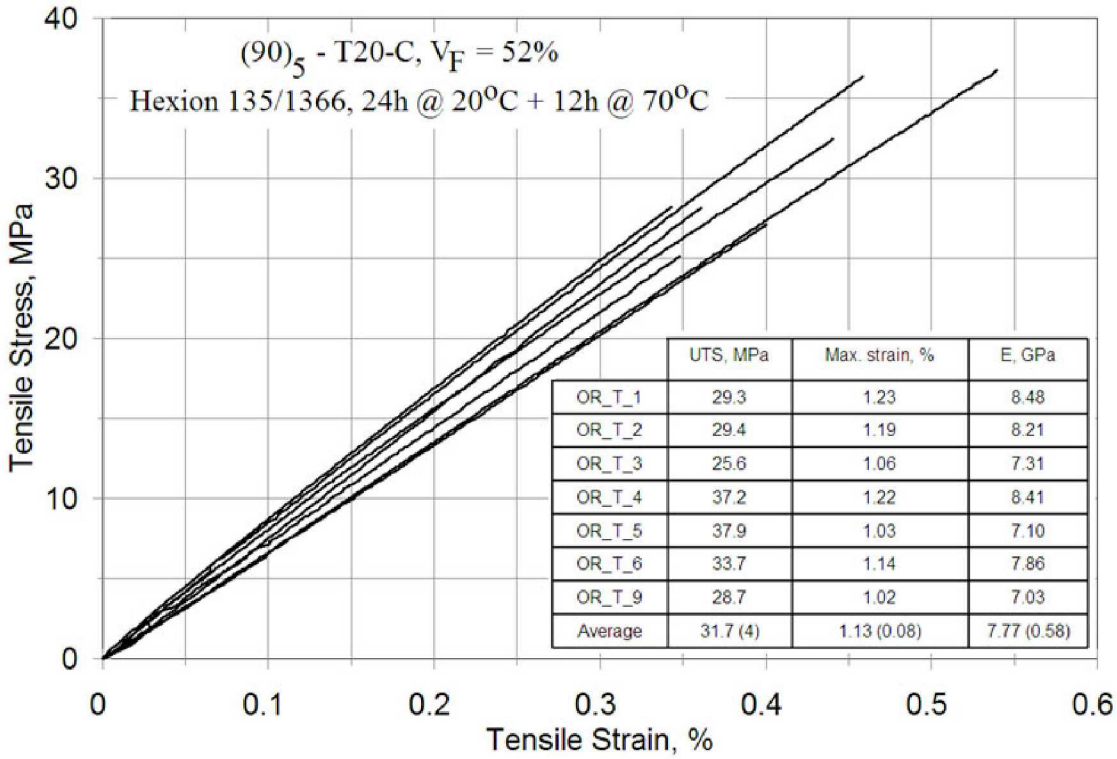

	UTS, MPa	Max. strain, %	E, GPa
OR_T_1	29.3	1.23	8.48
OR_T_2	29.4	1.19	8.21
OR_T_3	25.6	1.06	7.31
OR_T_4	37.2	1.22	8.41
OR_T_5	37.9	1.03	7.10
OR_T_6	33.7	1.14	7.86
OR_T_9	28.7	1.02	7.03
Average	31.7 (4)	1.13 (0.08)	7.77 (0.58)

Figure 3-12. Summary of $[90]_5$ transverse tension tests on the T20-C fiber plates.

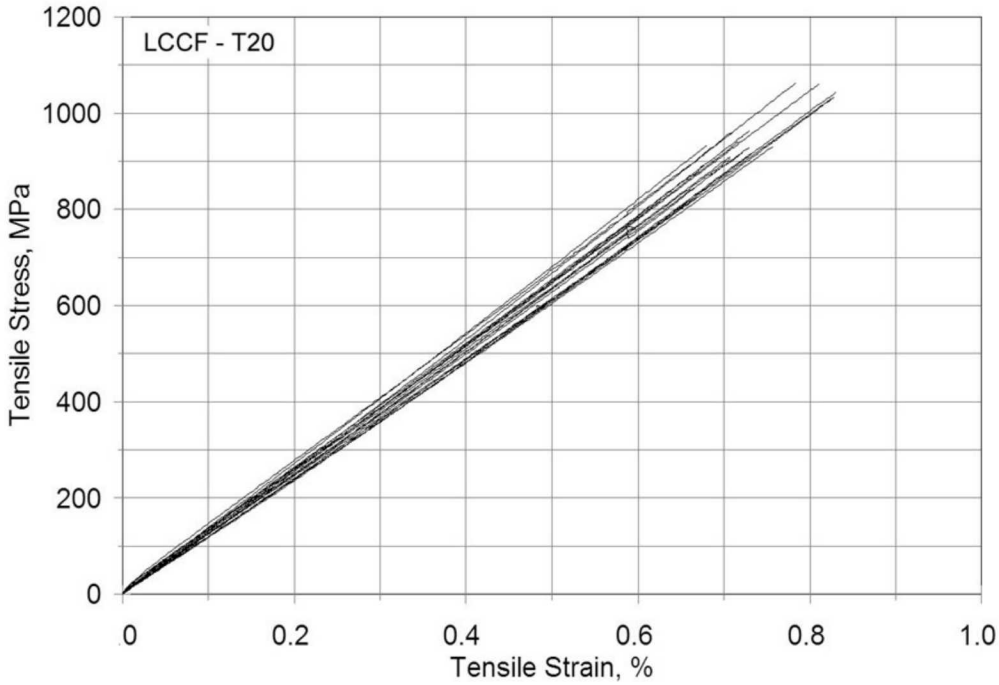

Figure 3-13. Summary of $[0]_3$ tensile tests on the T20-C fiber plates.

3.2.3. *Kaltex K20 Static Testing Results*

Figure 3-14 and Figure 3-15 show static stress-strain results for the Kaltex precursor composites. These coupons also lack damage accumulation, or stiffness loss, before final fracture. Further testing could investigate this phenomenon in future tests, as well as the unique fracture pattern of the coupons.

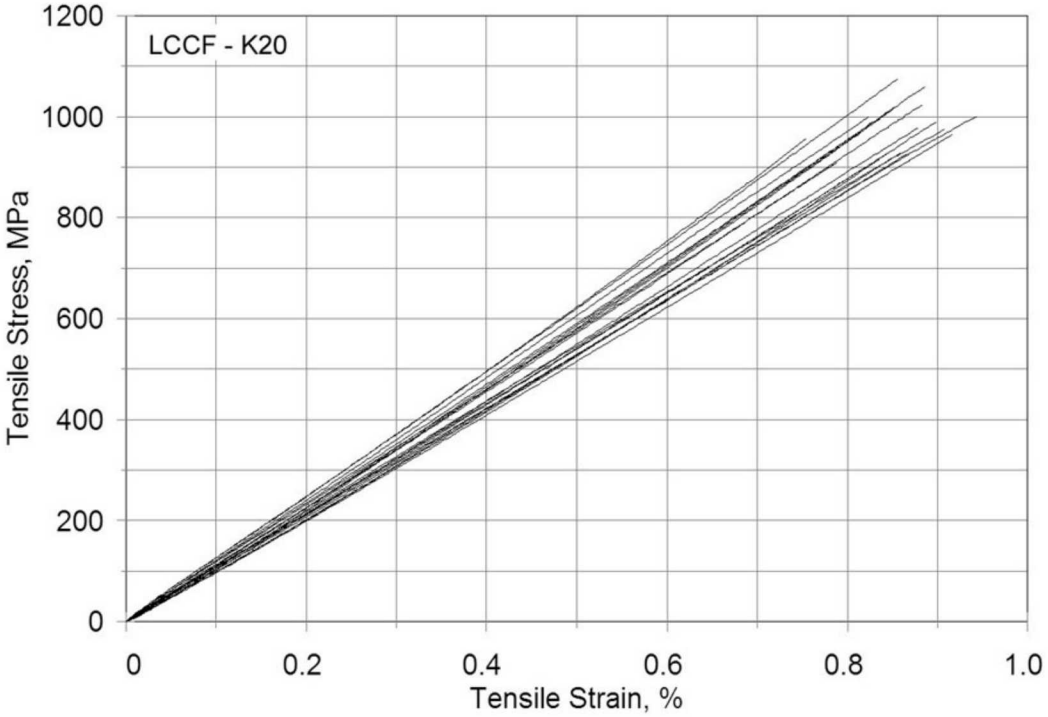

Figure 3-14. Summary of tensile tests on the MSU infused K20-C fiber plates.

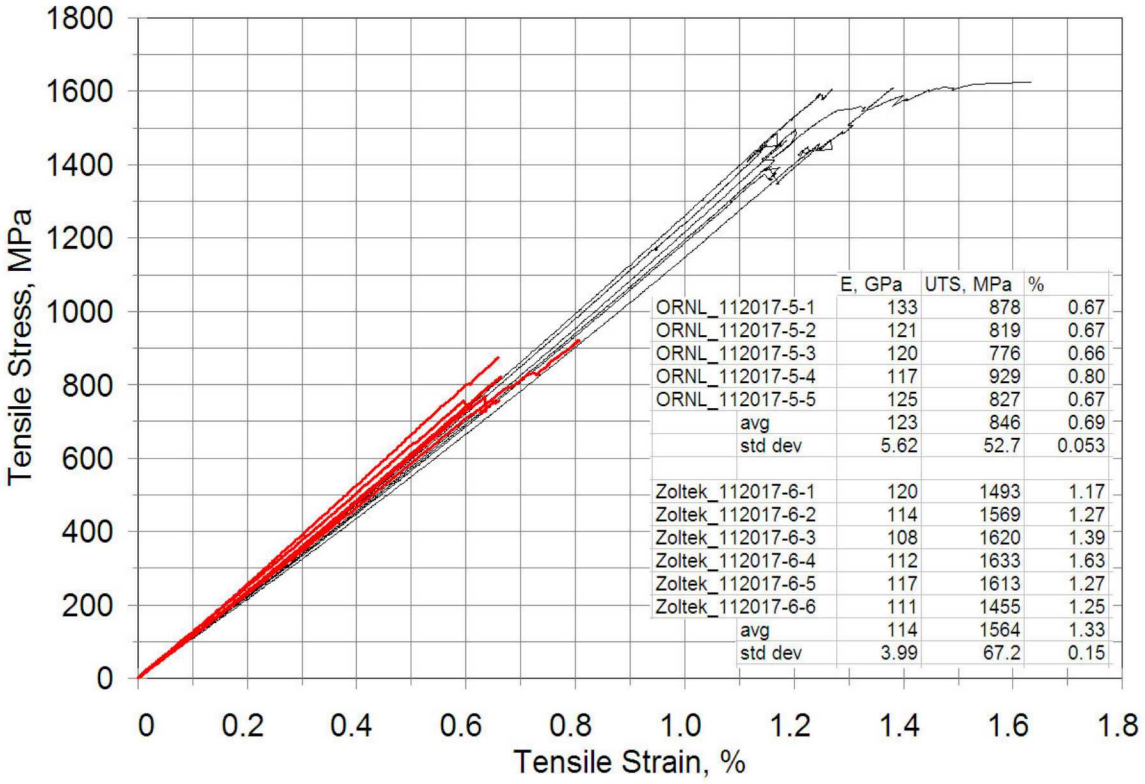

	E, GPa	UTS, MPa	%
ORNL_112017-5-1	133	878	0.67
ORNL_112017-5-2	121	819	0.67
ORNL_112017-5-3	120	776	0.66
ORNL_112017-5-4	117	929	0.80
ORNL_112017-5-5	125	827	0.67
avg	123	846	0.69
std dev	5.62	52.7	0.053
Zoltek_112017-6-1	120	1493	1.17
Zoltek_112017-6-2	114	1569	1.27
Zoltek_112017-6-3	108	1620	1.39
Zoltek_112017-6-4	112	1633	1.63
Zoltek_112017-6-5	117	1613	1.27
Zoltek_112017-6-6	111	1455	1.25
avg	114	1564	1.33
std dev	3.99	67.2	0.15

Figure 3-15. Summary of tensile tests on the supplied pultruded 112017-5 and 112017-6 laminates.

3.2.4. Fatigue Testing Results

A summary of the fatigue results is shown in Figure 3-16 for Zoltek PX35 pultrusion coupons and infused Taekwang and Kaltex coupons. Summary data of these fatigue tests are included in Table A-8 through Table A-10. These tests were run in tension-tension fatigue with stress ratio R=0.1. The higher single cycle tensile strain is due to both material differences and a higher fiber volume fraction for the Zoltek PX35 material in pultruded composite form.

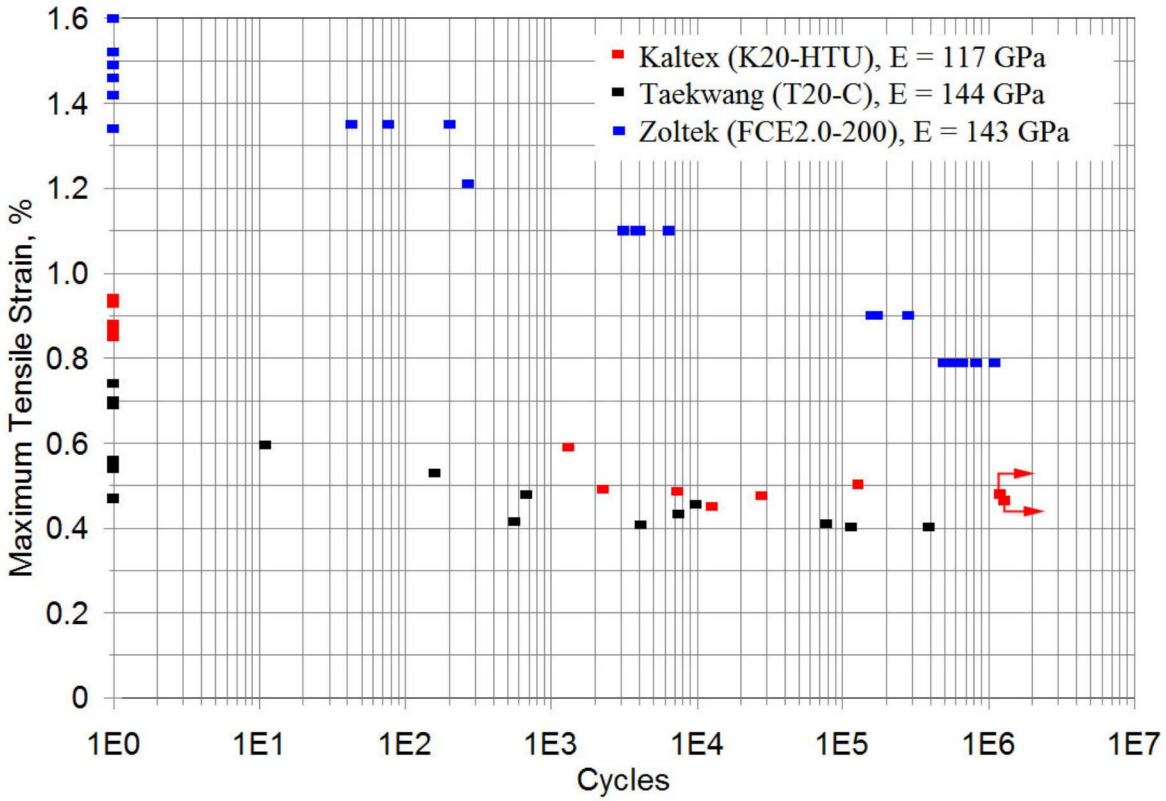

Figure 3-16. Summary of initial maximum strain versus cycles for the three materials, R=0.1.

4. DISCUSSION

The mechanical test results provide a broad overview and comparison of the CFTF heavy tow, textile carbon fiber materials and the Zoltek commercial product of PX35. These results include multiple manufacturing processes resulting in various forms of coupons; however, this also introduces some inconsistencies with resin properties, fiber volume fractions, and defect structures.

The summary test results in Table 2-4 provides the best illustration of the data comparison for these systems. From these data sets, very similar values of modulus were attained for similar manufacturing processes. More specifically, for tensile coupons manually aligned and infused with the same resin system, PX35, T20-C, and K20-HTU, had volume fractions of 52%, 52%, and 47% and moduli of 126 MPa, 124 MPa, and 112 MPa, respectively. Tensile strength values for the PX35 fibers did show a significant increase over the LCCF systems for MSU infused coupons, with PX35, T20-C, and K20-HTU strengths of 1726 MPa, 978 MPa and 990 MPa, respectively. This lower tensile strength for the LCCF fibers is observed across fabrication methods and resin systems, strongly indicating that the LCCF fibers do not indeed have the tensile strength of PX35, which is concurrent with tensile tow test data. However, the compressive strength for the PX35, T20-C, and K20-HTU MSU infused coupons were -906 MPa, -869 MPa, and -863 MPa, respectively, demonstrating very similar compressive strength properties for the materials, which is more critical for wind turbine blade design.

Another observation from the tensile tests is shown in Figure 4-1. The failed coupons from both CFTF systems showed very unique failure mechanisms. The Zoltek coupons (Zoltek-pultruded coupons are shown) show the typical "brooming" seen in all the PX35 coupons. This failure mode is primarily identified as the result of the compressive stress wave that travels through coupon at ultimate load, thus generating fiber failure near the grips and fiber splintering along the coupon length. However, the LCCF coupons show a very different failure surface. The coupons splinter and fracture into multiple pieces, with a very distinct angled fracture surface along the coupon. No "brooming" is seen. Inspection of the fracture surfaces have not yielded any valuable data as to why this system shows this unique, but repeatable, failure mechanism.

The fatigue data shown in Figure 3-16 illustrates a message similar to the static data for the LCCF systems. The LCCF systems show reduced static strength, but the fatigue life of the system is not affected. The PX35 composites tested did also have a higher fiber volume fraction (commercial pultrusion) which shifts its fatigue curve upwards. The LCCF systems appear to be less fatigue sensitive than the Zoltek PX35 pultruded system, with a potential intersection of the two systems near 10^7 cycles. The low fatigue insensitivity for the LCCF is a very positive result for use in wind turbine blades.

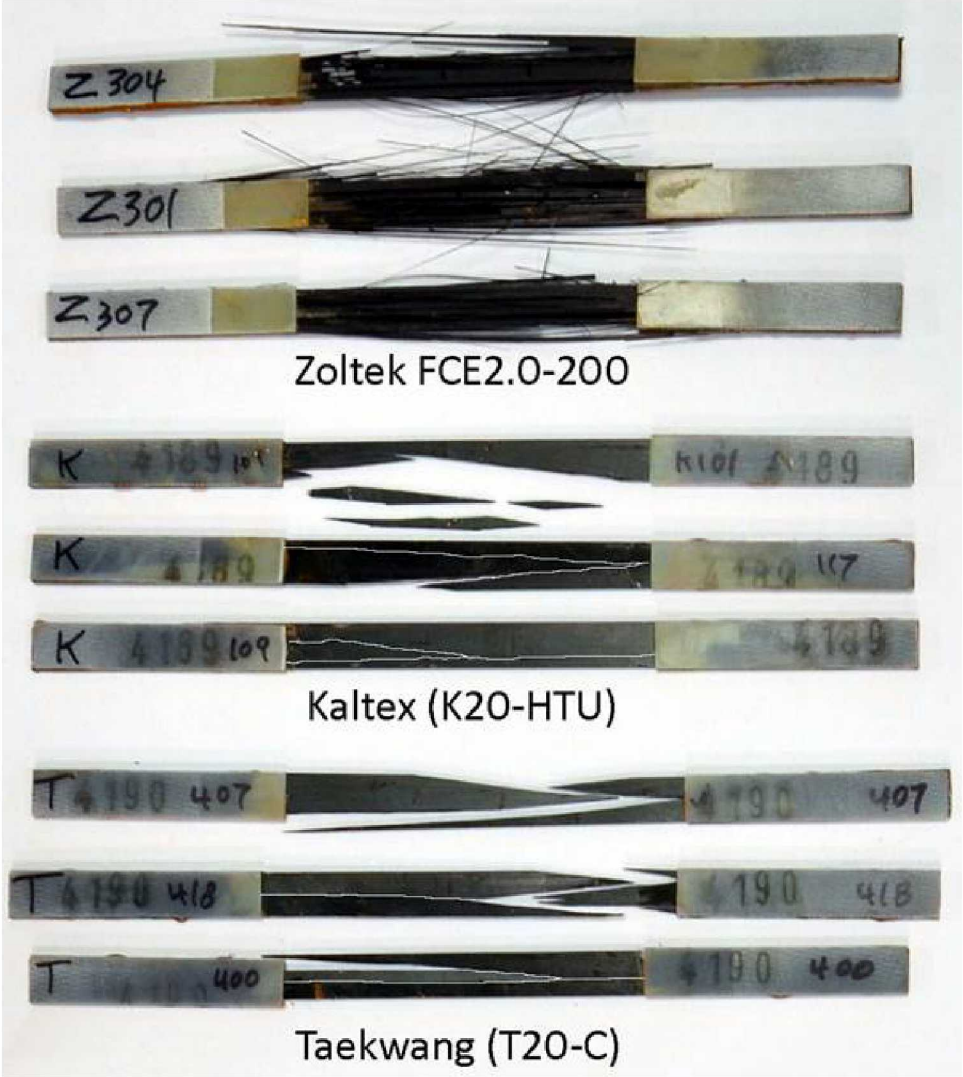

Figure 4-1. Failed tensile coupons of MSU infused LCCF fibers and Zoltek pultruded coupons.

REFERENCES

[1] Ennis, B.L., Kelley, C.K., Naughton, B.T., Norris, R.E., Das, S., Lee, D. and Miller, D.A., "*Optimized Carbon Fiber Composites in Wind Turbine Blade Design,*" Tech. Rep., Sandia National Laboratories, forthcoming 2019.

[2] ASTM E4 – 16 Standard Practices for Force Verification of Testing Machines

[3] ASTM E74-18e1 Standard Practices for Calibration and Verification for Force-Measuring Instruments

[4] ASTM E83 - 16 Standard Practice for Verification and Classification of Extensometer Systems

[5] ASTM E251 - 92(2014) Standard Test Methods for Performance Characteristics of Metallic Bonded Resistance Strain Gages

[6] Mandell, JF, Samborsky, DD, Agastra, P, Sears, AT and Wilson, TJ, "Analysis of SNL/MSU/DOE Fatigue Database Trends for Wind Turbine Blade Materials," Sandia Contractor Report SAND2010-7052, 2010

[7] ASTM D6641 / D6641M - 16e1 Standard Test Method for Compressive Properties of Polymer Matrix Composite Materials Using a Combined Loading Compression (CLC) Test Fixture

APPENDIX A. DETAILED TESTING RESULTS

This appendix lists the individual coupon results for researchers interested in recreating, replotting, or statistically interrogating the data. All data, except developmental test results, are also included in the SNL/MSU/DOE Composite Materials Database, http://windpower.sandia.gov/materials-reliability.

Substantial effort was given within this project to produce repeatable data consistent with the most accurate representation of the tested properties of materials. This required iteration of testing methods used but did not include optimization of material processing. To prevent the improper use of the summarized data, a few notes are made here. The testing method for the Zoltek pultruded plates in compression was iterated upon within this project, but early test results are included which have lower values than are representative of the material properties (both shown in Table A-6). The MSU infused Zoltek composites displayed reduced compressive properties in Table A-5 from what is expected (particularly when compared with the pultruded plates) and the composite manufacturing system is not considered to be optimized for this material.

Table A-1. Summary of tensile tests on the T20-C fiber using Hexion 135/1366 resin (shown in Figure 3-13).

Lay-up	Coupon	UTS, MPa	Max. strain, %	E, GPa
$[0]_5$	T20C-0-1	906	0.73	130
	T20C-0-2	1014	0.85	117
	T20C-0-3	1007	0.76	122
	T20C-0-4	961	0.76	118
	T20C-0-5	1004	0.80	119
$[0]_3$	T20-400	943	0.72	126
	T20-401	910	0.71	125
	T20-402	966	0.73	128
	T20-403	967	0.71	131
	T20-404	1066	0.81	125
	T20-405	884	0.68	130
	T20-406	1067	0.78	131
	T20-407	898	0.68	134
	T20-408	926	0.72	124
	T20-409	1035	0.83	119
	T20-410	1048	0.83	125
	T20-411	918	0.73	125
	T20-412	913	0.71	125
	T20-413	1035	0.83	121
	T20-414	924	0.73	122
	T20-415	934	0.76	119
	T20-416	895	0.71	129
	T20-417	881	0.73	125

Table A-2. Summary of tensile tests on the MSU infused K20-C $[0]_3$ lay-up using Hexion 135/1366 resin (shown in Figure 3-14).

Coupon	E, GPa	UTS, MPa	Max. Strain, %
K20-600	114	1018	0.85
K20-601	114	913	0.79
K20-602	108	898	0.73
K20-603	119	1004	0.82
K20-604	105	931	0.87
K20-605	104	930	0.79
K20-606	117	1063	0.89
K20-607	105	995	0.90
K20-608	116	1032	0.86
K20-609	109	977	0.91
K20-610	117	990	0.83
K20-611	118	991	0.82
K20-612	106	975	0.90
K20-613	123	957	0.70
K20-614	114	1027	0.88
K20-615	105	1002	0.94
K20-616	106	1037	0.86
K20-617	122	1080	0.86
Average	112	990	0.84
Std. Dev.	6	49	0.06

Table A-3. Summary of individual tow PX-35 longitudinal [0] tensile tests.

Lay-up	Coupon	UTS, MPa	Max. strain, %	E, GPa
5.1 tows/cm	PX35-4122-1	1556	1.42	119
	PX35-4122-2	1742	1.45	125
	PX35-4122-3	1669	1.63	116
	PX35-4122-4	1771	1.41	116
	PX35-4122-6	1767	1.53	114
	PX35-4122-10	1851	1.4	122
Single Tow	PX35-T2	2142	1.58	115
	PX35-T5	2092	1.63	113
	PX35-T7	2279	1.60	135
	PX35-T9	2220	1.63	131
	PX35-T10	2231	1.52	136

Table A-4. Summary of individual pultruded longitudinal [0] tensile tests.

Lay-up	Coupon	UTS, MPa	Max. strain, %	E, GPa
[0] pultruded	112017-5-1	878	0.67	133
	112017-5-2	819	0.67	121
	112017-5-3	776	0.66	120
	112017-5-4	929	0.80	117
	112017-5-5	827	0.67	125
[0] pultruded	FCE2-200-1	2222	1.34	149
	FCE2-200-2	2149	1.46	139
	FCE2-200-3	2373	1.60	142
	FCE2-200-4	2162	1.49	141
	FCE2-200-6	2157	1.52	140
	FCE2-200-10	2228	1.42	139
[0] pultruded	112017-6-1	1493	1.17	120
	112017-6-2	1569	1.27	114
	112017-6-3	1620	1.39	108
	112017-6-4	1633	1.63	112
	112017-6-5	1613	1.27	117
	112017-6-6	1455	1.25	111

Table A-5. Summary of individual MSU infused longitudinal [0] compressive tests.

Lay-up	Coupon	UTS, MPa	Max. strain, %	E, GPa	Back out UCS, MPa
$[0]_5$	T20C-0-31	-601	-0.53	113	
	T20C-0-32	-531	-0.37	143	
	T20C-0-33	-588	-0.51	117	
$[0]_{20}$	T20-450	-940	-0.75		
	T20-451	-822	-0.66		
	T20-452	-911	-0.73		
	T20-453	-830	-0.66		
	T20-454	-830	-0.66		
	T20-455	-862	-0.69		
	T20-456	-797	-0.64		
	T20-457	-912	-0.73		
	T20-458	-918	-0.73		
	T20-459	-871	-0.69		
$[0/90]_{3S}$	T20C-0-90-01	-475	-0.66	68.5	-894
	T20C-0-90-02	-503	-0.75	67.3	-946
	T20C-0-90-03	-495	-0.78	66.5	-930
	T20C-0-90-04	-453			-852
	T20C-0-90-05	-448			-842
$[0]_{20}$	K20-440	-787	-0.70		
	K20-441	-798	-0.71		
	K20-442	-758	-0.68	111	
	K20-444	-809	-0.72	113	
	K20-446	-988	-0.88		
	K20-447	-1039	-0.93		
[0]	PX35-4197-C1	-907	-0.74	123	
	PX35-4197-C2	-893	-0.73	123	
	PX35-4197-C3	-839	-0.67	126	
	PX35-4197-C4	-948	-0.78	121	
	PX35-4197-C5	-943	-0.76	125	

Table A-6. Summary of individual pultruded longitudinal [0] compressive tests.

Lay-up	Coupon	UTS, MPa	Min. strain, %	E, GPa	Back out UCS, MPa
[0] pultruded	FCE2-200-1C	-857	-0.63	132	
	FCE2-200-2C	-840	-0.66	132	
	FCE2-200-3C	-914	-0.64	145	
	FCE2-200-4C	-856	-0.68	130	
	FCE2-200-5C	-935	-0.55	152	
[0] pultruded	FCE2.0-200-Z1X-100	-1555	-1.20		
	FCE2.0-200-Z1X-101	-1449	-1.11		
	FCE2.0-200-Z1X-102	-1546	-1.19		
	FCE2.0-200-Z1X-103	-1518	-1.17		
	FCE2.0-200-Z1X-104	-1515	-1.24	127	
	FCE2.0-200-Z1X-105	-1529	-1.28	135	
	FCE2.0-200-Z1X-106	-1473	-1.23	130	
	FCE2.0-200-Z1X-107	-1458	-1.22	135	
[0] pultruded	112017-4C1	-830	-0.67		
	112017-4C2	-767	-0.62		
	112017-4C4	-811	-0.66		
[0] pultruded	112017-5C1	-713	-0.58		
	112017-5C2	-782	-0.64		
	112017-5C3	-699	-0.57		
	112017-5C4	-883	-0.72		
[0] pultruded	112017-6C1	-874	-0.77		
	112017-6C2	-1041	-0.91		
	112017-6C3	-835	-0.73		
	112017-6C4	-894	-0.78		
	112017-6C5	-853	-0.75		
	112017-6C6	-887	-0.78		

Table A-7. Summary of individual transverse [90] tensile tests.

Lay-up	Coupon	UTS, MPa	Max. strain, %	E, GPa
[90] pultruded	FCE2.0-200-ZT1	45.8	0.52	9.17
	FCE2.0-200-ZT2	52.9	0.60	9.24
	FCE2.0-200-ZT3	57.1	0.68	9.10
	FCE2.0-200-ZT4	60.3	0.74	8.96
	FCE2.0-200-ZT5	33.9	0.37	8.96
	FCE2.0-200-ZT6	47.7	0.54	9.17
	FCE2.0-200-ZT7	52.7	0.60	9.31
$[90]_5$	T20C-90-1	29.3	0.34	8.48
	T20C-90-2	29.4	0.36	8.21
	T20C-90-3	25.6	0.35	7.31
	T20C-90-4	37.2	0.46	8.41
	T20C-90-5	37.9	0.54	7.10
	T20C-90-6	33.7	0.44	7.86
	T20C-90-9	28.7	0.40	7.03
[90] pultruded	112017-4T1	10.0		
	112017-4T2	9.46		
	112017-4T3	12.6		
	112017-4T4	9.58		
	112017-4T5	8.46		
	112017-4T6	11.0		
[90] pultruded	112017-5T1	7.66		
	112017-5T2	7.65		
	112017-5T3	8.93		
	112017-5T4	8.26		
	112017-5T5	7.86		
[90] pultruded	112017-6T1	55.6		
	112017-6T2	58.3		
	112017-6T3	59.1		
	112017-6T4	55.1		
	112017-6T5	63.1		
[90] pultruded	112017-6T6	33.7		
	112017-6T7	31.7		
	112017-6T8	30.3		
	112017-6T9	31.4		
	112017-6T10	33.1		

Table A-8. Summary of static and fatigue tests containing Taekwang (T20-C) fiber, $[0]_5$ layup.

Coupon	UTS, MPa	R-value	Freq, Hz	E, GPa	Max. strain, %	Cycles to Failure	Comments
T4190-411	753	static	0.0254 mm/s	156	0.47	1	
T4190-421	946	static	0.0254 mm/s	135	0.69	1	
T4190-418	989	static	0.0254 mm/s	116	0.7	1	
T4190-420	767	static	0.0254 mm/s	134	0.56	1	
T4190-414	985	static	0.0254 mm/s	129	0.74	1	
T4190-401	862	0.1	1	169	0.56	1	
T4190-402	716	0.1	1	132	0.54	1	
T4190-400	862	0.1	1	140	0.6	11	
T4190-404	793	0.1	1	152	0.53	160	
T4190-407	690	0.1	2	165	0.42	563	
T4190-413	690	0.1	2	142	0.48	680	
T4190-415	621	0.1	2	151	0.41	4130	
T4190-423	621	0.1	2	140	0.43	7528	
T4190-408	690	0.1	2	151	0.46	9768	
T4190-417	552	0.1	3	131	0.41	77843	
T4190-412	552	0.1	2	135	0.4	115530	
T4190-422	552	0.1	3	135	0.4	394498	

Table A-9. Summary of static and fatigue tests containing Kaltex (K20-HTU) fiber K20, $[0]_5$ layup.

Coupon	UTS, MPa	R-value	Freq, Hz	E, GPa	Max. strain, %	Cycles to Failure	Comments
K4189-113	813	static	0.0254 mm/s	68.4	0.85	1	
K4189-111	980	static	0.0254 mm/s	76.1	0.88	1	
K4189-122	974	static	0.0254 mm/s	74.9	0.86	1	
K4189-116	1090	static	0.0254 mm/s	80.5	0.93	1	
K4189-101	929	static	0.0254 mm/s	95.0	0.94	1	
K4189-118	621	0.1	2.5	104	0.59	1333	
K4189-119	586	0.1	2	115	0.49	2296	
K4189-109	586	0.1	2	119	0.49	7387	
K4189-105	621	0.1	2.5	141	0.45	12770	
K4189-124	586	0.1	2	121	0.48	28180	
K4189-117	621	0.1	2.5	122	0.50	128006	
K4189-107	483	0.1	2	95.3	0.48	1200000	Runout
K4189-108	552	0.1	3	116	0.47	1300000	Runout

Table A-10. Summary of static and fatigue tests with pultruded Zoltek FCE2.0-200, V_F = 62%.

Coupon	UTS, MPa	R-value	Freq, Hz	E, GPa	Max. strain, %	Cycles to Failure	Comments
FCE2.0-003	2373	static	0.0254 mm/s	142	1.6	1	
FCE2.0-004	2162	static	0.0254 mm/s	141	1.5	1	
FCE2.0-005	2157	static	0.0254 mm/s	140	1.5	1	
FCE2.0-000	2228	static	0.0254 mm/s	139	1.4	1	
FCE2.0-001	2222	static	0.0254 mm/s	149	1.3	1	
FCE2.0-002	2149	static	0.0254 mm/s	139	1.5	1	
FCE2.0-314	2069	0.1	1	140	1.4	43	
FCE2.0-315	2069	0.1	1	141	1.4	77	
FCE2.0-312	2069	0.1	1	140	1.4	203	
FCE2.0-317	1896	0.1	1	139	1.2	270	
FCE2.0-329	1724	0.1	1.5	142	1.1	3139	
FCE2.0-326	1724	0.1	1.5	141	1.1	3844	
FCE2.0-328	1724	0.1	1.5	143	1.1	4050	
FCE2.0-309	1724	0.1	1	140	1.1	6424	
FCE2.0-316	1379	0.1	1.5	143	0.9	159714	
FCE2.0-308	1379	0.1	1.5	142	0.9	171529	
FCE2.0-320	1379	0.1	1.5	142	0.9	283219	
FCE2.0-350	1207	0.1	2	142	0.79	498795	
FCE2.0-321	1207	0.1	2	143	0.79	602187	
FCE2.0-325	1207	0.1	2	144	0.79	661029	
FCE2.0-310	1207	0.1	2	146	0.79	821465	
FCE2.0-300	1207	0.1	2	142	0.79	1111726	

DISTRIBUTION

Email—Internal

Name	Org.	Sandia Email Address
Technical Library	01177	libref@sandia.gov

Sandia National Laboratories

Sandia National Laboratories is a multimission laboratory managed and operated by National Technology & Engineering Solutions of Sandia LLC, a wholly owned subsidiary of Honeywell International Inc. for the U.S. Department of Energy's National Nuclear Security Administration under contract DE-NA0003525.